Available online at www.sciencedirect.com
SCIENCE DIRECT
Journal of Sound and Vibration 296 (2006) 1000–1012
JOURNAL OF SOUND AND VIBRATION
www.elsevier.com/locate/jsvi

Love waves in double porosity media

Zhi-jun Dai, Zhen-Bang Kuang*

Department of Engineering Mechanics, Shanghai Jiaotong University, Shanghai 200240, PR China

Received 9 February 2005; received in revised form 14 March 2006; accepted 17 March 2006
Available online 2 June 2006

Abstract

Based on the control equations for double-porosity media extended from Biot's theory, the propagation of Love waves is discussed in this paper. Dispersion equations of Love waves in double porosity medium are obtained by utilizing the usual assumption of Love waves in elastic solid with the coupling mass coefficient ρ_{23} and coupling permeability term $k^{(12)}$ being equal to zero. The dispersion and attenuation properties of Love waves in double porosity medium are analyzed. The approximate limit of the Love wave speed is also given. The effects of fracture porosity and fracture permeability on the behavior of the propagation of Love waves are investigated in detail.

1. Introduction

It has been confirmed that in some materials such as most rocks and some acoustic absorbent, there exist two kinds of main porosities. One is the matrix porosity, also called the storage porosity, occupying a substantial fraction of the total volume but having a very low permeability. The other is fracture or crack porosity, occupying very little volume but having a very high permeability. It is evident that the classical Biot theory [1,2] is not adequate to describe these materials due to the homogeneous assumption of the porosity. The relevant problems such as the consolidation and dynamic response of double porosity medium have received more and more attention in recent years. The double porosity theory has been applied in various fields such as oil extraction, geological exploration and water resources exploitation. The double porosity model was first proposed by Barrenblatt [3] to express fluid flow in hydrocarbon reservoirs and aquifers. Warren and Root [4] made an improvement to this model, which allows for coupling between the rock deformation and the fluid flow. Aifantis [5,6] constructed a general double porosity theory of consolidation in the framework of mixture theory. Wilson and Aifantis [7] studied the wave propagation in a saturated fractured porous medium without detailed derivations. Their analysis showed that there exist three compressional and one rotational waves, in which the first and the third compressional waves are similar to the fast and slow compressional waves in Biot's theory, and the second compressional wave arises due to the presence of fractures. The second compressional wave is dispersive and highly damped. Based on Aifantis's double porosity model Bescos and his co-workers [8–11] published a series of papers to investigate the

*Corresponding author. Tel.: +86 021 54743067; fax: +86 021 54743044.
E-mail address: zbkuang@mail.sjtu.edu.cn (Z.-B. Kuang).

0022-460X/$ - see front matter © 2006 Elsevier Ltd. All rights reserved.
doi:10.1016/j.jsv.2006.03.029

dynamic behavior of fissured poroelastic rocks extensively. More explicit and detailed equations of motion were presented, and the effect of the porosity and permeability parameters on the characteristics of four bulk waves and Rayleigh waves was discussed in detail. In addition the frequency correction for double porosity model in high frequency range is also given. A comparative study between double porosity theory and single porosity model was also presented. According to the mixture theory, Tuncay and Corapcioglu [12,13] use the volume averaging technique to investigate wave propagation in a fractured porous medium saturated by two immiscible fluids based on the double-porosity approach. Berryman and Wang [14,15] derived the phenomenological equations for double porosity media and presented the method to determine the relevant coefficients.

It is well known that Loves waves play an important role in the seismology, geophysics and earthquake engineering. At present, the properties of Love waves in single porosity medium have been studied by many researchers based on the Biot's theory. Deresiewicz [16,17] discussed Loves waves in a porous layer overlaying on elastic half-space and in a porous layer between two elastic half-space. Sharma and Gogna [18] considered Love waves in a slow elastic layer lying on a porous half-space with an initial stress. Wang and Zhang [19] discussed the propagation of Love waves in a transversely isotropic fluid-saturated porous layered half-spaced in detail, and gave dispersion and attenuation curves. Liu and De Boer [20] considered Love waves within a saturated porous layer overlaying a homogeneous, isotropic half-space, and discussed the effects of permeability parameters on velocity and attenuation.

It has been confirmed that the double porosity and dual permeability model is more suitable to describe the materials containing two kinds of main pores. The purpose of this paper is to discuss the propagation of Love waves in a double porosity medium filled with one kind of incompressible fluid. Balance equations and constitutive relations constructed by Berryman and Wang [15] are adopted. The general analytical method utilized by Wang and Zhang [19] in their study of the same problem in single porosity medium is followed here. More complicated characteristic equations of Love waves are obtained. The organization of this paper is as follows. In Section 2, the controlling equations of double porosity media are reviewed. The dispersion relations of Love waves in a homogeneous isotropic double porosity layer overlying a homogeneous isotropic double porosity half-space are derived. In Section 3, based on the dispersion equations derived in Section 2, numerical calculations are performed. The upper and lower bounds of the Love wave speeds are also given. The dispersion curves of Love wave speed and group speed are plotted. In Section 4 some conclusions are given.

2. Basic equations

Consider a double porosity layer with the thickness H overlaying a double porosity half-space as shown in Fig. 1. X, Y and Z denote the rectangular Cartesian coordinates and Y orients in the direction perpendicular and outward to the paper. Both the layer and the half-space are supposed to be homogeneous and isotropic materials. In the following sections, the double porosity medium is composed of the matrix and fracture pores, and the matrix itself is composed of the solid material and matrix pores.

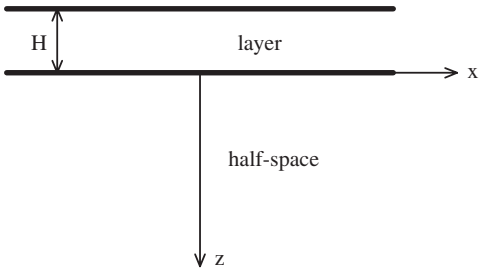

Fig. 1. A schematic drawing of the problem.

2.1. Wave motion equations

Since Love waves belong to an antiplane and shear motion, the nonzero displacement components are only u_y, $U_y^{(1)}$ and $U_y^{(2)}$. Therefore, the equations of motion can be expressed as [15]:

$$\begin{pmatrix} \rho_{11} & \rho_{12} & \rho_{13} \\ \rho_{12} & \rho_{22} & \rho_{23} \\ \rho_{13} & \rho_{23} & \rho_{33} \end{pmatrix} \begin{pmatrix} \ddot{u}_y \\ \ddot{U}_y^{(1)} \\ \ddot{U}_y^{(2)} \end{pmatrix} + \begin{pmatrix} b_{12}+b_{13} & -b_{12} & -b_{13} \\ -b_{12} & b_{12}+b_{23} & -b_{23} \\ -b_{13} & -b_{23} & b_{13}+b_{23} \end{pmatrix} \begin{pmatrix} \dot{u}_y \\ \dot{U}_y^{(1)} \\ \dot{U}_y^{(2)} \end{pmatrix} = \begin{pmatrix} \sigma_{yj,j} \\ -\bar{p}_{,y}^{(1)} \\ -\bar{p}_{,y}^{(2)} \end{pmatrix} \tag{1}$$

where u_y, $U_y^{(1)}$ and $U_y^{(2)}$ are the solid displacement, matrix pore fluid displacement and fracture pore fluid displacement, respectively, ρ_{ij} and b_{ij} are shown in Appendix. The superimposed dot "$\cdot$" denotes the differentiation with respect to time t. The index i refers to one of the three Cartesian coordinates X, Y, Z, and a comma before a subscript indicates the derivative with respect to the indicated coordinate direction. $\bar{p}^{(1)}$and $\bar{p}^{(2)}$ are macroscopic fluid pressures, related to the internal fluid pressures $p^{(1)}$ and $p^{(2)}$ in the matrix pore and fracture pore respectively, by

$$\bar{p}^{(1)} = v^{(1)}\phi^{(1)}p^{(1)}, \quad \bar{p}^{(2)} = v^{(2)}p^{(2)}, \tag{2}$$

where $v^{(1)}$ and $v^{(2)}$ are volume fractions of the matrix and fracture pore, respectively, with $v^{(1)}+v^{(2)}=1$, $\phi^{(1)}$ is the volume fraction of the matrix pore in the matrix and the volume fraction of the matrix pore in the medium is $v^{(1)}\phi^{(1)}$. Thus the genaral porosity can be expressed as

$$\phi = v^{(1)}\phi^{(1)} + v^{(2)}. \tag{3}$$

Let $k^{(11)}$, $k^{(12)}$,$k^{(21)}$,and $k^{(22)}$ are permeability coefficients and τ, $\tau^{(1)}$ and $\tau^{(2)}$ are overall, matrix and fracture tortuosity factors, respectively, and η is the shear viscosity of the fluid. The mass coefficients ρ_{ij} and coupling viscosity coefficients b_{ij} are listed in Appendix.

For the wave propagation, it will often be adequate to assume that the cross-coupling coefficients between the matrix pore and fracture are equal to zero, as this effect is presumably more important for the long-term drainage of fluid than it is for the short-term propagation of waves. Considering this approximation, we assume $k^{(12)}=k^{(21)}=0$, $\rho_{23}=0$ and $b_{23}=0$ in the following discussions.

The constitutive equations for double porosity media can be written in the form

$$\begin{pmatrix} \sigma_{11} \\ \sigma_{22} \\ \sigma_{33} \\ -p^{(1)} \\ -P^{(2)} \\ \sigma_{23} \\ \sigma_{31} \\ \sigma_{12} \end{pmatrix} = \begin{pmatrix} C_{11} & C_{12} & C_{13} & m_{14} & m_{15} & 0 & 0 & 0 \\ C_{21} & C_{22} & C_{23} & m_{24} & m_{25} & 0 & 0 & 0 \\ C_{31} & C_{32} & C_{33} & m_{34} & m_{35} & 0 & 0 & 0 \\ m_{41} & m_{42} & m_{43} & m_{44} & m_{45} & 0 & 0 & 0 \\ m_{51} & m_{52} & m_{53} & m_{54} & m_{55} & 0 & 0 & 0 \\ 0 & 0 & 0 & 0 & 0 & 2G & 0 & 0 \\ 0 & 0 & 0 & 0 & 0 & 0 & 2G & 0 \\ 0 & 0 & 0 & 0 & 0 & 0 & 0 & 2G \end{pmatrix} \begin{pmatrix} \varepsilon_{11} \\ \varepsilon_{22} \\ \varepsilon_{33} \\ -w^{(1)} \\ -w^{(2)} \\ \varepsilon_{23} \\ \varepsilon_{31} \\ \varepsilon_{12} \end{pmatrix}, \tag{4}$$

where C_{ij} s ($i, j = 1, 2, 3$ representing three Cartesian coordinates x, y and z, respectively) are drainage elastic moduli and G is shear modulus, m_{ij} s are material parameters, σ_{ij} s and ε_{ij} s are the solid stresses and strains, respectively. $w^{(1)}$ and $w^{(2)}$ are the increments of fluid in the matrix phase and fractures, respectively, given by

$$w^{(1)} = -v^{(1)}\phi^{(1)}\nabla\cdot(U^{(1)}-u), \quad w^{(2)} = -v^{(2)}\nabla\cdot(U^{(2)}-u). \tag{5}$$

The time harmonic variations for the displacements in the solid, fluid in matrix pores and fluid in fractures may be written as

$$u_y = f(z)\mathrm{e}^{i(kx-\omega t)}, \quad U_y^{(1)} = g_1(z)\mathrm{e}^{i(kx-\omega t)}, \quad U_y^{(2)} = g_2(z)\mathrm{e}^{i(kx-\omega t)}. \tag{6}$$

Substituting Eq. (4) into Eq. (1) and considering Eqs. (5), (6) and $\rho_{23} = b_{23} = 0$, the Love wave equation in double porosity medium can be obtained

$$-\omega^2 \begin{pmatrix} \omega^2\rho_{11} + i\omega(b_{12}+b_{13}) & \omega^2\rho_{12} - i\omega b_{12} & \omega^2\rho_{13} - i\omega b_{13} \\ \omega^2\rho_{12} - i\omega b_{12} & \omega^2\rho_{22} + i\omega b_{12} & 0 \\ \omega^2\rho_{13} - i\omega b_{13} & 0 & \omega^2\rho_{33} + i\omega b_{13} \end{pmatrix} \begin{pmatrix} f(z) \\ g_1(z) \\ g_2(z) \end{pmatrix} = \begin{pmatrix} G\frac{\partial^2 f(z)}{\partial z^2} + k^2 G f(z) \\ 0 \\ 0 \end{pmatrix}. \quad (7)$$

From Eq. (7) we can obtain a second-order partial derivative equation for $f(z)$:

$$\frac{\mathrm{d}^2 f(z)}{\mathrm{d}z^2} + \gamma^2 f(z) = 0. \quad (8)$$

The general solution of the above equation is

$$f(z) = r_1 \mathrm{e}^{i\gamma z} + r_2 \mathrm{e}^{-i\gamma z}, \quad (9)$$

$$g_1(z) = -\frac{\omega^2\rho_{12} - i\omega b_{12}}{\omega^2\rho_{22} + i\omega b_{12}} f(z), \quad g_2(z) = -\frac{\omega^2\rho_{13} - i\omega b_{13}}{\omega^2\rho_{33} + i\omega b_{13}} f(z), \quad (10)$$

where

$$\gamma^2 = -k^2 + \frac{i\omega(b_{12}+b_{13}) + \omega^2\rho_{11}}{G} - \frac{(-i\omega b_{12} + \omega^2\rho_{12})^2}{G(i\omega b_{12} + \omega^2\rho_{22})} - \frac{(-i\omega b_{13} + \omega^2\rho_{13})^2}{G(\omega^2\rho_{33} - i\omega b_{13})}. \quad (11)$$

Hence the solid displacements in the layer and half-space can be, respectively, expressed as

$$\bar{u}_y = (\bar{r}_1 \mathrm{e}^{i\bar{\gamma}z} + \bar{r}_2 \mathrm{e}^{-i\bar{\gamma}z})\mathrm{e}^{i(kx-\omega t)}, \quad u_y = r_1 \mathrm{e}^{i\gamma z}\mathrm{e}^{i(kx-\omega t)}, \quad (12)$$

where the superimposed bars "–" refer the quantities of the layer, $\bar{r}_1, \bar{r}_2$ and r_1 are constants determined by the boundary conditions.

2.2. Boundary conditions

For Love waves in the present problem, the boundary conditions are:

$$\begin{aligned} &u_y = \bar{u}_y, && z = 0, \\ &\sigma_{zy} = 0, && z = -H, \\ &\sigma_{zy} = \bar{\sigma}_{zy}, && z = 0, \\ &u_y = 0, && z \to \infty. \end{aligned} \quad (13)$$

To satisfy the last condition, we must have $\mathrm{Im}(\gamma) > 0$, $\mathrm{Re}(\bar{\gamma}) \neq 0$ (without loss of generality, it is assumed that $\mathrm{Re}(\bar{\gamma}) > 0$).

2.3. Dispersion equations

Generally the wavenumber in a porous medium can be written as

$$k = k_1(1 + i\delta), \quad (14)$$

where k_1 is the real part of the wavenumber, connected with the angular frequency ω and phase velocity c by $k_1 = \omega/c$, and δ is the attenuation coefficient. It is convenient to introduce the following contractions:

$$\begin{aligned} c_s &= \sqrt{G}\left[\rho_{11} + \frac{2b_{12}^2\rho_{12} + b_{12}^2\rho_{22} - \omega^2\rho_{12}^2\rho_{22}}{s_1} + \frac{2b_{13}^2\rho_{13} + b_{13}^2\rho_{33} - \omega^2\rho_{13}^2\rho_{33}}{s_2}\right]^{-\frac{1}{2}}, \\ \bar{c}_s &= \sqrt{\bar{G}}\left[\bar{\rho}_{11} + \frac{2\bar{b}_{12}^2\bar{\rho}_{12} + \bar{b}_{12}^2\bar{\rho}_{22} - \omega^2\bar{\rho}_{12}^2\bar{\rho}_{22}}{\bar{s}_1} + \frac{2\bar{b}_{13}^2\bar{\rho}_{13} + \bar{b}_{13}^2\bar{\rho}_{33} - \omega^2\bar{\rho}_{13}^2\bar{\rho}_{33}}{\bar{s}_2}\right]^{-\frac{1}{2}}, \end{aligned} \quad (15)$$

$$\delta_1 = \frac{\omega c_s^2}{2G}\left[\frac{b_{12}(\rho_{12}+\rho_{22})^2}{s_1} + \frac{b_{13}(\rho_{13}+\rho_{33})^2}{s_2}\right],$$
$$\bar{\delta}_1 = \frac{\omega \bar{c}_s^2}{2\bar{G}}\left[\frac{\bar{b}_{12}(\bar{\rho}_{12}+\bar{\rho}_{22})^2}{\bar{s}_1} + \frac{\bar{b}_{13}(\bar{\rho}_{13}+\bar{\rho}_{33})^2}{\bar{s}_2}\right], \tag{16}$$

where $s_1 = b_{12}^2 + \omega^2\rho_{22}^2$, $s_2 = b_{13}^2 + \omega^2\rho_{33}^2$, $\bar{s}_1 = \bar{b}_{12}^2 + \omega^2\bar{\rho}_{22}^2$, $\bar{s}_2 = \bar{b}_{13}^2 + \omega^2\bar{\rho}_{33}^2$.

Therefore γ and $\bar{\gamma}$ in Eq. (11) can be written in the form

$$\gamma = ik_1 q, \quad \bar{\gamma} = k_1 \bar{q}, \tag{17}$$

where

$$q = \left\{\left[(1-\delta^2) - \left(\frac{c}{c_s}\right)^2\right] + 2i\left[\delta - \delta_1\left(\frac{c}{c_s}\right)^2\right]\right\}^{\frac{1}{2}}, \tag{18}$$

$$\bar{q} = \left\{\left[\left(\frac{c}{\bar{c}_s}\right)^2 - (1-\delta^2)\right] + 2i\left[\bar{\delta}_1\left(\frac{c}{\bar{c}_s}\right)^2 - \delta\right]\right\}^{\frac{1}{2}}. \tag{19}$$

To satisfy the requirements of $\mathrm{Im}(\gamma)>0$ and $\mathrm{Re}(\bar{\gamma})>0$, we must have

$$\bar{c}_s\sqrt{1-\delta^2} < c < c_s\sqrt{1-\delta^2}. \tag{20}$$

Eq. (20) is the extension of the propagation of Love waves in the classical layered elastic medium. Generally $\delta << 1$ for SH waves, therefore the values of the upper and lower bounds of the Love wave speed c may approximately take c_s and $\bar{c}_s$, respectively.

Substituting Eq. (12) into boundary conditions (13), we obtain the dispersion equation

$$\tan(\bar{\gamma}H) = \frac{G\gamma}{i\bar{G}\bar{\gamma}} \text{ or } \tan(k_1\bar{q}H) = \frac{Gq}{\bar{G}\bar{q}}. \tag{21}$$

We further set:

$$\bar{q} = \bar{q}_1 + i\bar{q}_2, \quad \frac{Gq}{\bar{G}\bar{q}} = a + ib, \tag{22}$$

where $\bar{q}_1$, $\bar{q}_2$, a and b are all real.

Then Eq. (21), upon separation of the real and imaginary parts, yields two real equations:

$$\tan(\bar{q}_1 k_1 H) = \frac{a}{1 - b\,\tanh(\bar{q}_2 k_1 H)}, \tag{23}$$

$$\tanh(\bar{q}_2 k_1 H) = \frac{b}{1 + a\,\tan(\bar{q}_1 k_1 H)}. \tag{24}$$

Eqs. (23) and (24) can be solved by an iterative procedure [19]. Therefore, the dispersion curves (velocity c and group velocity $c_p$versus k_1H) and attenuation curves (Log (δ) versus k_1H) can be determined. It is noticed that the fluid pressure ($p^{(1)}$ or $p^{(2)}$) does not appear in the above equations. The group velocity c_p is the propagation velocity of energy for a dispersive wave, which is given by

$$c_p = \frac{\mathrm{d}\omega}{\mathrm{d}k_1} = c + k_1\frac{\mathrm{d}c}{\mathrm{d}k_1}. \tag{25}$$

It is noted that for an elastic medium, the attenuation coefficient δ equals zero, and the elastic medium do not contain fluid, so the fluid displacement terms, i.e., $U^{(1)}$ and $U^{(2)}$, are all equal to zero. Therefore, the coupling mass coefficientsρ_{12}, ρ_{13}, ρ_{22}, ρ_{23}, ρ_{33} all disappear in the motion equation. The only preserving mass coefficient is ρ_{11}, which equals to ρ, the density of the material composing the elastic half-space. Therefore, in the case that the half-space is elastic medium and the overlying layer is double porosity medium, the

expression of c_s in Eq. (15) can be reduced to $c_s = \sqrt{G/\rho}$. Correspondingly, the following condition should be satisfied:

$$\bar{c}_s\sqrt{1-\delta^2} < c < c_s,\ c_s = \sqrt{G/\rho}. \tag{26}$$

Similarly, in the case the overlying layer is elastic medium and the half-space is double porosity medium, we have

$$\bar{c}_s < c < c_s\sqrt{1-\delta^2}, \quad \bar{c}_s = \sqrt{\bar{G}/\bar{\rho}}. \tag{27}$$

When the layer and half-space are all elastic medium, Eqs. (18) and (19) are, respectively, reduced to

$$q = \left[1 - \left(\frac{c}{c_s}\right)^2\right]^{\frac{1}{2}}, \quad c_s = \sqrt{G/\rho}, \tag{28}$$

$$\bar{q} = \left[1 - \left(\frac{c}{\bar{c}_s}\right)^2\right]^{\frac{1}{2}}, \quad \bar{c}_s = \sqrt{\bar{G}/\bar{\rho}}. \tag{29}$$

3. Numerical results and discussions

Numerical calculations are performed for three situations: (a) an elastic layer overlays a double porosity half-space; (b) a double porosity layer overlays an elastic half-space; and (c) a double porosity layer overlays a double porosity half-space.

3.1. An elastic layer overlays a double porosity half-space.

The shear modulus of the layer and the mass density are taken to be

$$\bar{G} = 3\,\text{GPa}, \quad \bar{\rho}_s = 3000\,\text{kg/m}^3 \quad \text{and } \bar{c}_s = \sqrt{\bar{G}/\bar{\rho}_s} = 1000\,\text{m/s}. \tag{30}$$

The material constants of the double porosity half-space used in this paper are taken to

$$\begin{aligned} &G = 8\,\text{GPa}, \quad v^{(1)} = 0.9892, \quad v^{(2)} = 0.0108\\ &\phi^{(1)} = 0.1838, \quad \phi = 0.1926\\ &k^{(11)} = 10^{-16}\,\text{m}^2, \quad k^{(22)} = 10^{-12}\,\text{m}^2\\ &\rho_f = 1000\,\text{kg/m}^3, \quad \rho_s = 3000\,\text{kg/m}^3, \quad \eta = 10^{-3}\,\text{Pa s} \end{aligned} \tag{31}$$

For the above double porosity medium, the limiting value of wave velocity c_s can be calculated numerically and the curve of c_s as a function of f is plotted in Fig. 2. It is seen from Fig. 2 that c_s increases as the frequency increases and the variation of c_s is very gentle when the frequency is less than 200 Hz or larger than 4000 Hz. While the frequency is in the range about 300–4000 Hz, the variation of c_s is dramatic. When the frequency tends to zero and infinity, the limiting values of c_s are, respectively, given by

$$\begin{aligned} c_{s0} &= \sqrt{\frac{G}{\rho_{11}+2\rho_{12}+\rho_{22}+2\rho_{13}+\rho_{33}}} = 1627.98\,\text{m/s},\\ c_{s\infty} &= \sqrt{\frac{G\rho_{22}\rho_{33}}{\rho_{11}\rho_{22}\rho_{33}-\rho_{12}^2\rho_{33}-\rho_{13}^2\rho_{22}}} = 1703.65\,\text{m/s}. \end{aligned} \tag{32}$$

So the phase velocity is in the range $1000\,\text{m/s} < c < c_s(f)$.

The thickness of the elastic layer is taken as $H = 10$, 1 and 0.1 m, respectively. The dispersion curves (c and c_p versus k_1H) and attenuation curves are, respectively, illustrated in Figs. 3(a) and (b). (In the above and the

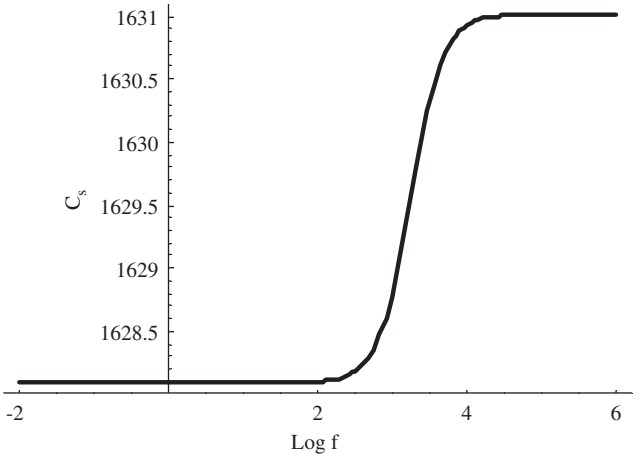

Fig. 2. Variations of c_s with material constants shown in Eq. (31) in a discussed double porosity medium with Log$f$.

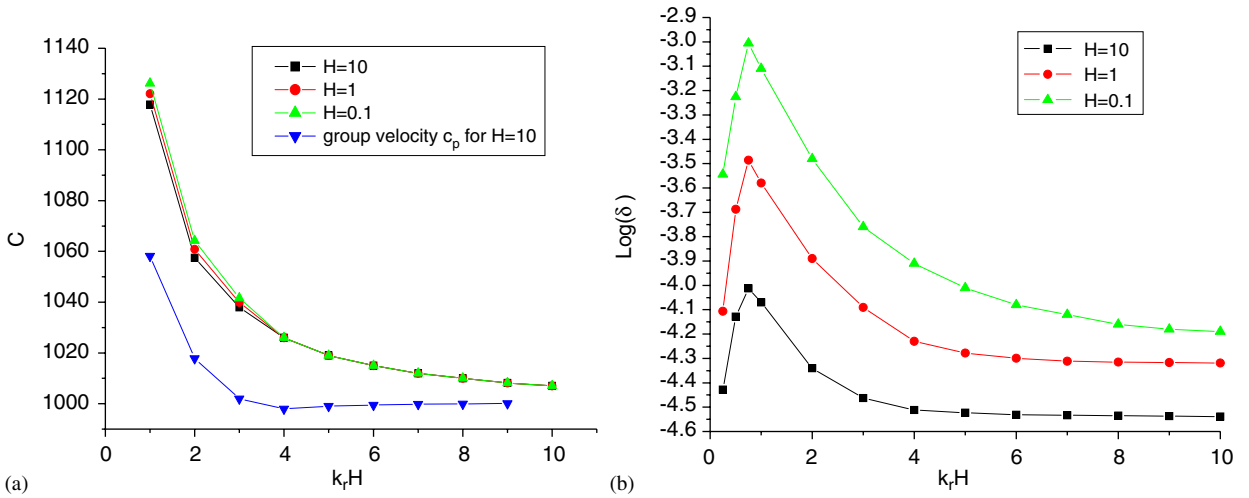

Fig. 3. (a) Wave speed versus k_1H at different thickness of the layer for case (a). The group speed verse k_1H is plotted according to Eq. (25) for $H = 10$. The material constants of the elastic layer and the double porosity half-space are given in Eqs. (30) and (31), respectively. (b) Attenuation versus k_1H at different thickness of the layer for case (a). The material constants are the same as in panel (a).

following figures, we only plot the first-order mode of Love waves.) It follows from figures that the velocity and attenuation of Love waves decreases rapidly at first and then slowly as k_1H increases, while the group velocity c_p decreases first and then increases as k_1H increases. Thus we can infer the group velocity c_p must reach a minimum value at some critical frequency, which varies with the thickness of the layer. For the case considered, values of the critical frequency are approximate 75 Hz for $H = 10$, 750 Hz for $H = 1$ and 7500 Hz for $H = 0.1$. At the critical frequency the energy of Love wave propagates most slowly. It is also shown in the figures that the thickness of the layer almost has no influence on phase velocity, but has evident influence on the attenuation. For the same k_1H, the thinner the elastic layer is, the larger the attenuation is.

In order to examine the effect of fracture permeability on the wave speed and attenuation, we take $k^{(22)}$ as 10^{-11}, 10^{-12}, 10^{-13} and $10^{-16}\,\mathrm{m}^2$, respectively. $H = 10\,\mathrm{m}$, $v^{(2)} = 0.0108$, and other material properties also keep constants. The calculation results are shown in Figs. 4(a) and (b). It is shown that the fracture permeability $k^{(22)}$ has a small influence on Love wave speed in the low frequency range. At the same k_1H, the smaller $k^{(22)}$ is, the bigger the phase velocity is. In high frequency range, for example $k_1H, > 6$ in Fig. 4(a), $k^{(22)}$

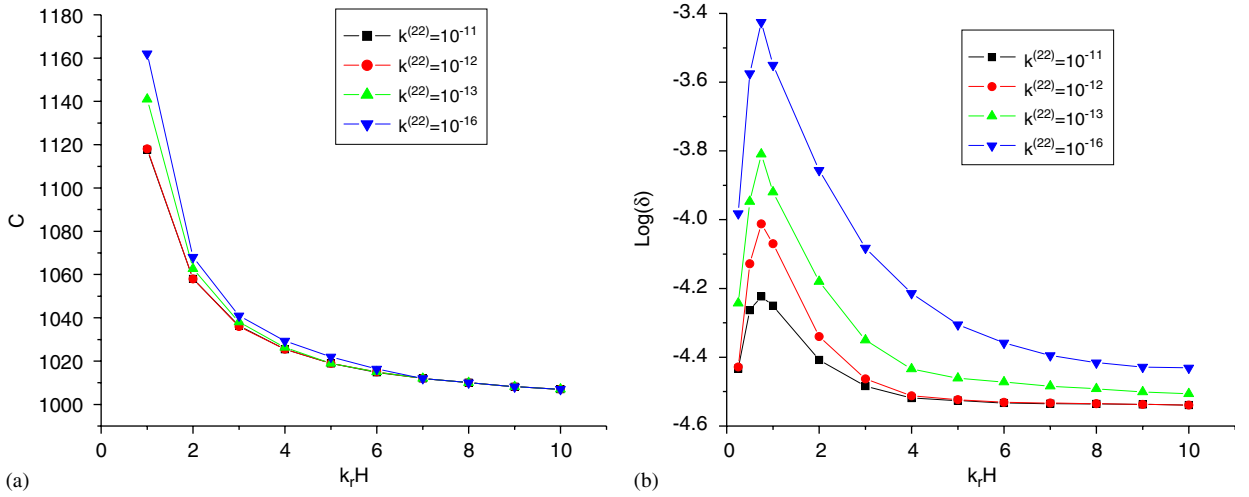

Fig. 4. (a) Wave speed versus k_1H at different fracture permeability ($k^{(22)}$) parameters of the double porosity half-space for case (a). The material constants are the same as in Fig. 3(a). (b) Attenuation versus k_1H at different fracture permeability ($k^{(22)}$) parameters of the double porosity half-space for case (a). The material constants are the same as in Fig. 3(a).

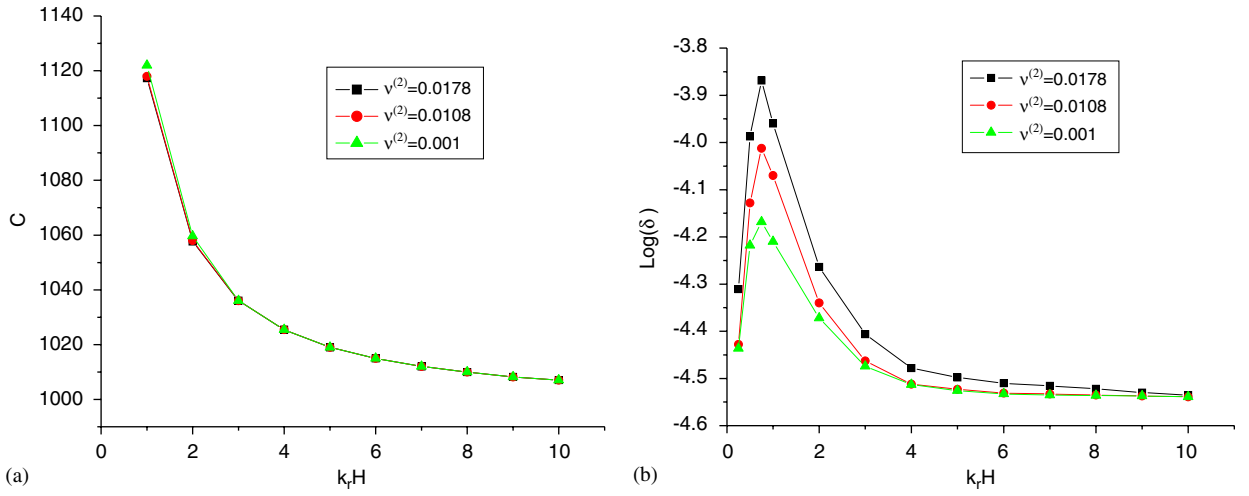

Fig. 5. (a) Wave speed versus k_1H at different fracture porosity ($v^{(2)}$) parameters for case (a). The material constants are the same as in Fig. 3(a). (b) Attenuation versus k_1H at different fracture porosity ($v^{(2)}$) parameters for case (a). The material constants are the same as in Fig. 3(a).

almost has no effect on phase velocity. Otherwise fracture permeability $k^{(22)}$ has relatively evident effect on the attenuation. At the same k_1H, the smaller $k^{(22)}$ is, the bigger the attenuation is.

Taking $H = 10\,\text{m}$, $k^{(22)} = 10^{-12}\,\text{m}^2$ and $v^{(2)}$ as 0, 0.001, 0.0108 and 0.0178, respectively, while the general porosity $\phi = 0.1926$ remains invariable, we discuss the effect of fracture porosity on the propagation of Love waves. Calculation results are shown in Figs. 5(a) and (b). It follows from these figures that the fracture porosity almost has no influence on the wave speed. The attenuation varies significantly with $v^{(2)}$ in low frequency range. For the same k_1H, the larger $v^{(2)}$ is, the larger the attenuation is. It can also be observed that the Love wave speed for single porosity medium ($v^{(2)} = 0$) is generally higher than the corresponding one for double porosity medium, while the attenuation for single porosity medium ($v^{(2)} = 0$) is generally lower than the corresponding one for double porosity medium and the difference is more evident as k_1H tend to zero.

3.2. A double porosity layer overlays an elastic half-space

The material constants of the elastic half-space are taken to be

$$G = 12\,\text{GPa}, \quad \rho_s = 3000\,\text{kg/m}^3 \quad \text{and } c_s = \sqrt{G/\rho_s} = 2000\,\text{m/s}. \tag{33}$$

The material constants of the layer are listed in Eq. (31). So the phase velocity is in the range $\bar{c}_s(f) < c < 2000\,\text{m/s}$, where $\bar{c}_s$ is the same as c_s shown in Fig. 2.

Similar to case (a), we also discuss the effect of the thickness of the layer H, fracture permeability $k^{(22)}$ and fracture porosity $v^{(2)}$ on Love wave propagation. Calculation results are shown, respectively, in Figs. 6–8.

It is shown in Figs. 6(a) and (b) that the velocity of Love waves and the group speed decrease rapidly at first and then slowly as k_1H increases. There is also a minimum value for group velocity c_p at some critical

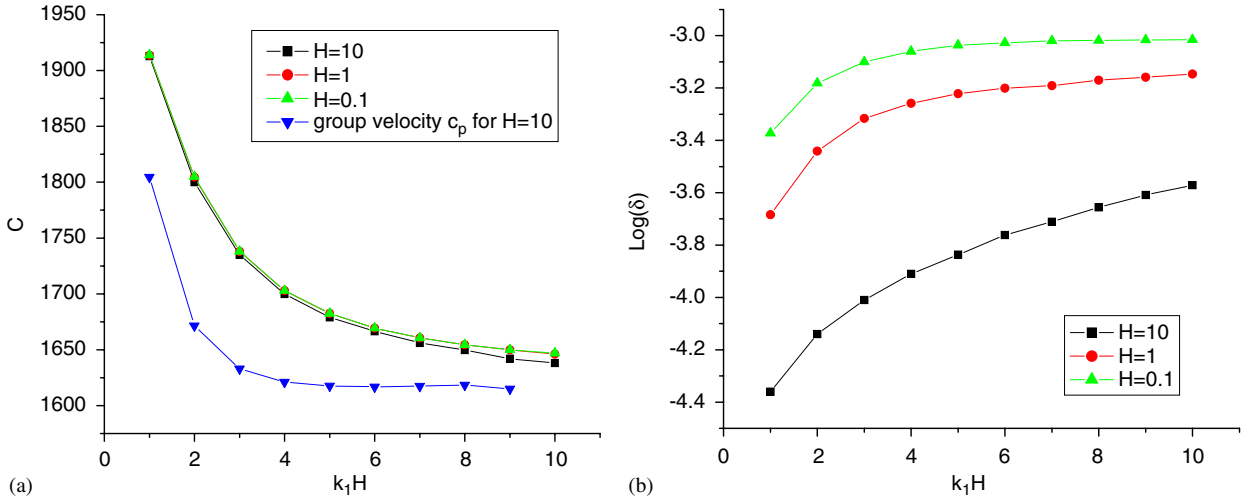

Fig. 6. (a) Wave speed versus k_1H at different thickness of the layer for case (b). The group speed verses k_1H is also plotted according to Eq. (25) for $H = 10$. The material constants of the double porosity layer and the elastic half-space are given in Eqs. (31) and (33), respectively. (b) Attenuation versus k_1H at different thickness of the layer for case (b). The material constants are the same as in panel (a).

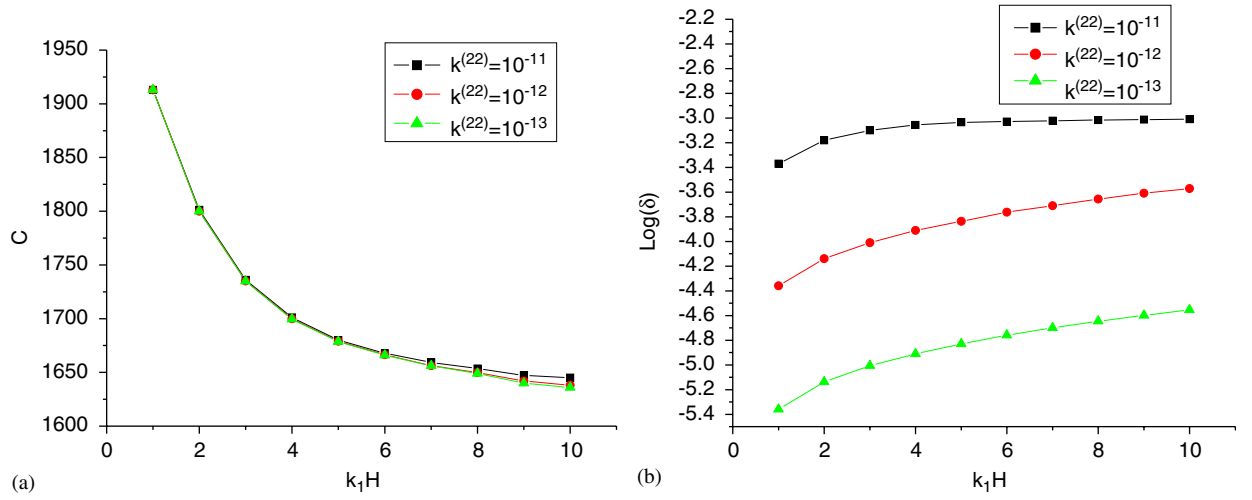

Fig. 7. (a) Wave speed versus k_1H at different fracture permeability ($k^{(22)}$) parameters of the double porosity layer for case (b). The material constants are the same as in Fig. 6(a). (b) Attenuation versus k_1H at different fracture permeability ($k^{(22)}$) parameters of the double porosity layer for case (b). The material constants are the same as in Fig. 6(a).

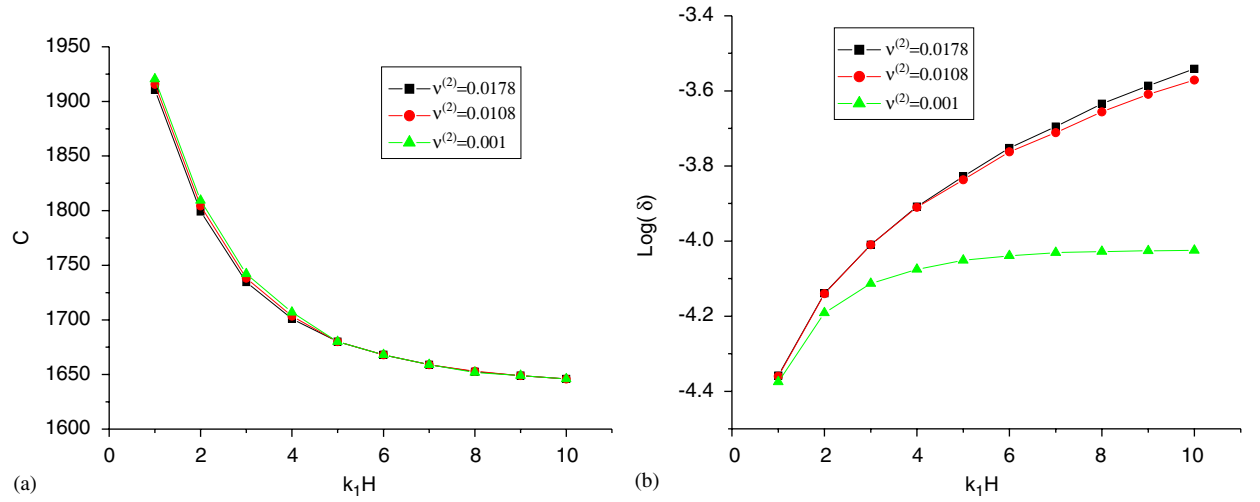

Fig. 8. (a) Wave speed versus k_1H at different fracture porosity ($v^{(2)}$) parameters of the double porosity layer for case (b). The material constants are the same as in Fig. 6(a). (b) Attenuation versus k_1H at different fracture porosity ($v^{(2)}$) parameters of the double porosity layer for case (b). The material constants are the same as in Fig. 6(a).

frequency. The thickness H of the layer almost has no effect on velocity in low frequency range, but has small influence on velocity in high frequency range. For the same k_1H, the thinner the layer is, the larger the velocity is. The attenuation increases rapidly at first and then slowly as k_1H increases. For the same k_1H, the thinner the double porosity layer is, the larger the attenuation is. Comparing Figs. 3(b) and (b), it is found that the variation of attenuation with k_1H are opposite in the two cases.

It follows from Figs. 7(a) and (b) that the fracture permeability $k^{(22)}$ almost has no influence on Love wave speed in all the frequency range considered, while the attenuation varies greatly with $k^{(22)}$. At the same k_1H, the bigger the fracture permeability $k^{(22)}$ is, the larger the attenuation is.

From Figs. 8(a) and (b), we can see that the Love wave speed almost remains invariable as fracture porosity $v^{(2)}$ changes, while the attenuation varies greatly with $v^{(2)}$, especially in high frequency range. The larger the fracture porosity is, the larger the attenuation is. It can also be seen from figures that in this case the Love wave speed for single porosity medium ($v^{(2)} = 0$) is generally higher than the corresponding one for double porosity medium, which is similar to case (a). The attenuation for single porosity medium ($v^{(2)} = 0$) is generally lower than the corresponding one for double porosity medium and the difference is more evident as the frequency increases.

3.3. A double porosity layer overlays a double porosity half-space

The material constants of the half-space are taken to be:

$$G = 12\,\text{GPa}, \quad v^{(1)} = 0.9905, \quad v^{(2)} = 0.0095, \quad \phi^{(1)} = 0.1848, \quad \phi = 0.15,$$
$$k^{(11)} = 10^{-16}\,\text{m}^2, \quad k^{(22)} = 10^{-12}\,\text{m}^2,$$
$$\rho_f = 1000\,\text{kg/m}^3, \quad \rho_s = 3000\,\text{kg/m}^3, \quad \eta = 10^{-3}\,\text{Pa s}. \tag{34}$$

The material constants of the overlying layer are taken to be the same as Eq. (31). In this case $\bar{c}_{s0} = 1627.98\,\text{m/s}$, $\bar{c}_{s\infty} = 1703.65\,\text{m/s}$, and $c_{s0} = 2056.95\,\text{m/s}$, $c_{s\infty} = 2180.95\,\text{m/s}$. Since both the layer and the half-space are double porosity medium, here we only discuss the effect of the thickness of the layer on phase velocity and attenuation. Similar to the above cases, the thickness of the layer is taken as $H = 10$, 1 and 0.1 m, respectively. Fig. 9(a) shows the variation of phase velocity with frequency. As expected, the phase velocity decreases as the frequency increases. It is shown that contrasting the above two cases, the thickness of the layer obviously affect the Love wave speed, especially in low frequency range. At the same frequency, the Love wave

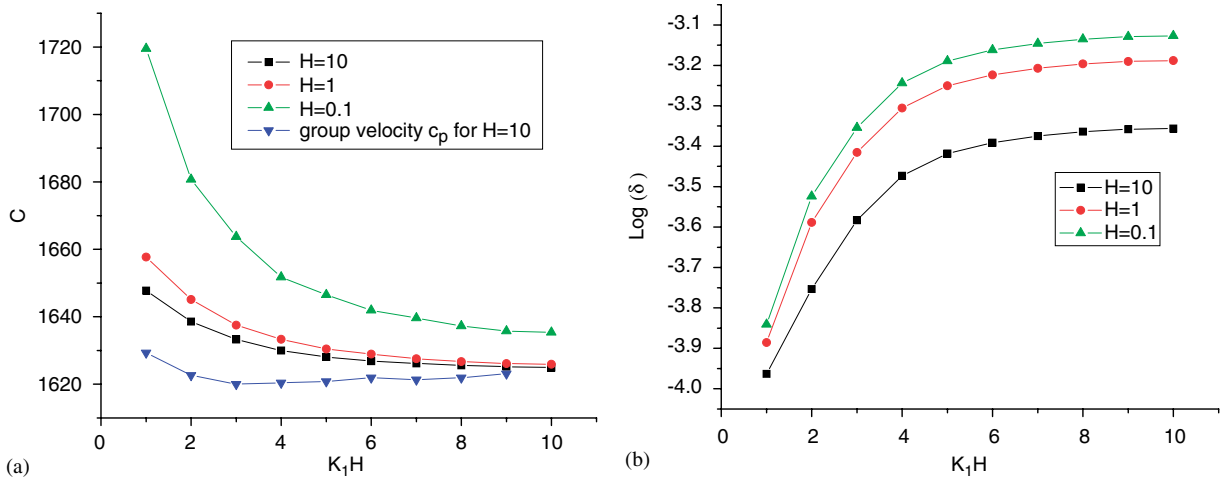

Fig. 9. (a) Wave speed versus k_1H at different thickness of the layer for case (c). The group speed verse k_1H is also plotted according to Eq. (25) for $H = 10$. The material constants of the double porosity layer and the double porosity half-space are given in Eqs. (31) and (34), respectively. (b) Attenuation versus k_1H at different thickness of the layer for case (c). The material constants are the same as in Fig. 9(a).

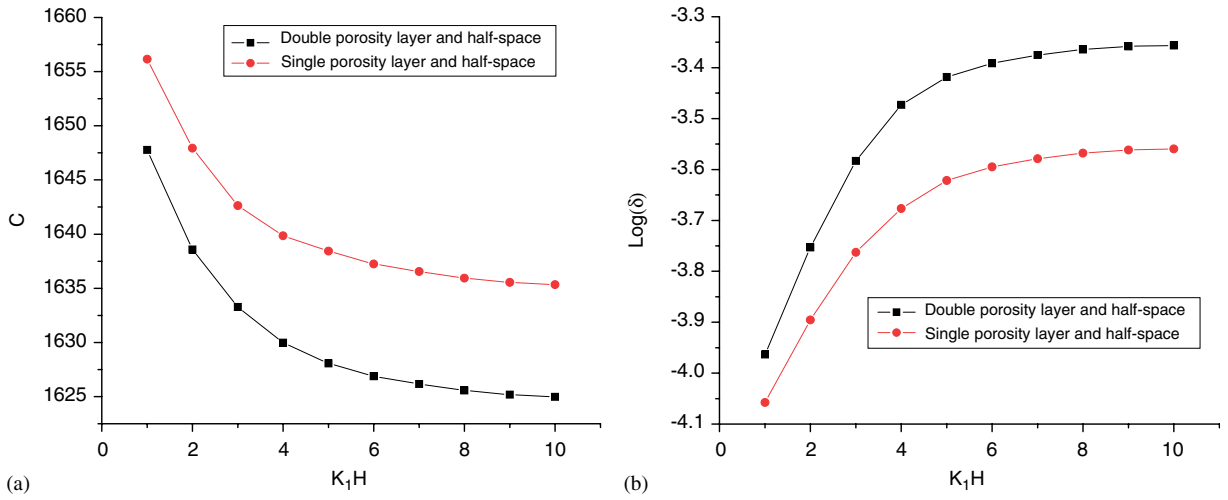

Fig. 10. (a) Comparison of the Love wave speed for double porosity layer/half-space with that for single-porosity layer/half-space; (b) comparison of the attenuation of Love waves for double porosity layer/half-space with that for single-porosity layer/half-space.

speed increases as the thickness of the layer H decreases. In addition, group speeds are also calculated. It is found that just like case (a) and (b), there is also a critical frequency at which the group speed reaches a minimum value. Attenuation of Love waves as a function of k_1H is shown in Fig. 9(b). It follows from the figure that the attenuation increases as the frequency increases, which is somewhat similar to the case (b). At the same frequency, the thicker the layer is, the lower the attenuation is.

Numerical calculations are also performed when the layer and the half-space are all fluid-saturated single porosity medium by taking the fracture porosity $v^{(2)} = 0$ (the general porosity remains invariable). $H = 10$ and other parameters remain constants. Calculation results are shown in Figs. 10(a) and (b). It is found that in general the Love wave speed for single-porosity medium is higher than that for double porosity medium while the attenuation of Love waves for single-porosity medium is lower than that for double porosity medium. The difference between two cases is more evident as the frequency increases.

4. Summary and conclusions

In the present paper, a theoretical analysis has been developed to study the propagation of Love waves in a double porosity medium. The phase velocity and dispersion equation are derived. Three cases are discussed in detail with numerical examples. It is found that the fluid pressure $p^{(1)}$ and $p^{(2)}$ do not appear in the dispersion equation. Therefore, the values of the fluid pressure have no influence on the propagation of Love waves in double porosity media. The approximate limits of Love waves are given, i.e., $\bar{c}_s\sqrt{1-\delta^2} < c < c_s\sqrt{1-\delta^2}$. Generally Love waves in a double porosity medium are highly dispersive, especially in low frequency range, and weakly damped (δ is less than 10^{-3} for the three cases considered above). Variations of the limiting value of the Love wave speed in a double porosity medium with frequency (c_s versus f) are very gentle when the frequency is less than 200 Hz or larger than 4000 Hz. The limiting values of c_s in low and high frequency range are, respectively,

$$\sqrt{\frac{G}{\rho_{11}+2\rho_{12}+\rho_{22}+2\rho_{13}+\rho_{33}}} \quad \text{and} \quad \sqrt{\frac{G\rho_{22}\rho_{33}}{\rho_{11}\rho_{22}\rho_{33}-\rho_{12}^2\rho_{33}-\rho_{13}^2\rho_{22}}}.$$

Numerical calculations reveal that the fracture permeability, fracture porosity and the thickness of the layer have important influence on the attenuation but only have very little influence on the phase velocity for case (a) and (b). It is found that the Love wave speed for single-porosity layer/half-space is higher than that for double porosity medium while the attenuation of Love waves for single-porosity medium is lower than that for double porosity layer/half-space in general and the difference between two cases is more evident as the frequency increases. Comparing the case (a) and (b), we also found that the variation of attenuation with k_1H is opposite. While for case (c) the thickness of the layer has significant influence on both the wave speed and the attenuation. Thinner the layer is, the larger the wave speed and the attenuation are. It is also found that there exists a critical frequency at which the group velocity reaches a minimum value, and this critical frequency is dependent on the thickness of the layer.

Acknowledgments

The financial support from National Natural Scientific Foundation of China under Grant No. 10132010 10472069 is gratefully acknowledged.

Appendix

The mass coefficients ρ_{ij} and the coupling viscosity coefficients b_{ij} are given as follows:

$$\rho_{11} = (1-\phi)\rho_s + (\tau-1)\phi\rho_f,$$

$$\rho_{12} = \frac{[(\tau^{(2)}-1)v^{(2)} - (\tau^{(1)}-1)v^{(1)}\phi^{(1)} - (\tau-1)\phi]\rho_f}{2},$$

$$\rho_{13} = \frac{[(\tau^{(1)}-1)v^{(1)}\phi^{(1)} - (\tau^{(2)}-1)v^{(2)} - (\tau-1)\phi]\rho_f}{2},$$

$$\rho_{22} = \tau^{(1)}v^{(1)}\phi^{(1)}\rho_f,$$

$$\rho_{23} = \frac{[(\tau-1)\phi - (\tau^{(1)}-1)v^{(1)}\phi^{(1)} - (\tau^{(2)}-1)v^{(2)}]\rho_f}{2},$$

$$\rho_{33} = \tau^{(2)}v^{(2)}\rho_f,$$

$$b_{12} = \frac{\eta(1-\tau^{(2)})\phi^{(1)}[v^{(1)}\phi^{(1)}k^{(22)} - v^{(2)}k^{(21)}]\rho_f}{k^{(11)}k^{(22)} - k^{(12)}k^{(21)}},$$

$$b_{13} = \frac{\eta(v^{(2)})^2}{k^{(22)}},$$

$$b_{23} = \frac{\eta v^{(1)}v^{(2)}\phi^{(1)}k^{(12)}}{k^{(11)}k^{(22)} - k^{(12)}k^{(21)}}.$$

References

[1] M.A. Biot, Theory of propagation of elastic waves in a fluid-saturated porous solid. I. Low frequency range. II. Higher frequency range, *Journal of the Acoustical Society of America* 28 (1955) 168–191.

[2] M.A. Biot, Mechanics of deformation and acoustic propagation in porous media, *Journal of Applied Physics* 33 (1962) 1482–1498.

[3] G.I. Barenblatt, I.P. Zheltow, T.N. Kochina, Basic concepts in the theory of seepage homogeneous liquids in fissured rocks, *Journal of Applied Mathematics and Mechanics* 24 (1960) 1286–1303.

[4] J.E. Warren, P.J. Root, The behavior of naturally fractured reservoirs, *Society of Petroleum Engineering Journal* 3 (1963) 245–255.

[5] E.C. Aifantis, On the problem of diffusion in solids, *Acta Mechanica* 37 (1980) 265–296.

[6] R.K. Wilson, E.C. Aifantis, On the theory of consolidation with double porosity, *International Journal of Engineering Science* 20 (1982) 1009–1035.

[7] R.K. Wilson, E.C. Aifantis, A double porosity model for acoustic wave propagation in fractured-porous rock, *International Journal of Engineering Science* 22 (1984) 1209–1217.

[8] D.E. Beskos, Dynamics of saturated rocks, I: equations of motions, *Journal of Engineering Mechanics ASCE* 115 (1989) 982–995.

[9] D.E. Beskos, I. Vgenopoulou, C.P. Providakis, Dynamics of saturated rocks, II: body waves, *Journal of Engineering Mechanics ASCE* 115 (1989) 996–1106.

[10] D.E. Beskos, C.N. Papadakis, H.S. Woo, Dynamics of saturated rocks, III: Rayleigh waves, *Journal of Engineering Mechanics ASCE* 115 (1989) 1017–1034.

[11] I. Vgenopoulou, D.E. Beskos, Dynamics of saturated rocks, IV: column and borehole problems, *Journal of Engineering Mechanics ASCE* 118 (1992) 1795–1813.

[12] K. Tuncay, M.Y. Corapcioglu, Body waves in fractured porous media saturated by two immiscible Newtonian fluids, *Transport in Porous Media* 13 (1996) 259–273.

[13] K. Tuncay, M.Y. Corapcioglu, Wave propagation in fractured porous media, *Transport in Porous Media* 23 (1996) 237–258.

[14] J.G. Berryman, H.F. Wang, The elastic coefficients of double-porosity models for fluid transport in jointed rock, *Journal of Geophysical Research* 100 (1995) 34611–34627.

[15] J.G. Berryman, H.F. Wang, Elastic wave propagation and attenuation in a double-porosity dual-permeability media, *International Journal of Rock Mechanics and Mining Science* 37 (2000) 63–78.

[16] H. Deresiewicz, The effects of boundaries on wave propagation in a liquid filled porous solid: II Love waves in a porous layer, *Bulletin of the Seismological Society of America* 51 (1961) 51–59.

[17] H. Deresiewicz, The effects of boundaries on wave propagation in a liquid filled porous solid: IX Love waves in a porous internal stratum, *Bulletin of the Seismological Society of America* 54 (1964) 919–923.

[18] M.D. Sharma, M.L. Gogna, Propagation of Love waves in an initially stressed medium consisting of a slow elastic layer lying over a liquid-saturated porous solid half-space, *Journal of the Acoustical Society of America* 89 (1991) 2584–2588.

[19] Y.-S. Wang, Z.-M. Zhang, Propagation of Love waves in a transversely isotropic fluid-saturated porous layered half-space, *Journal of the Acoustical Society of America* 103 (2) (1998) 695–701.

[20] Z.F. Liu, R. De Boer, Dispersion and attenuation of surface waves in a fluid-saturated porous medium, *Transport in Porous Media* 29 (1997) 207–223.